Cellulose (2025) 32:295–311
https://doi.org/10.1007/s10570-024-06282-0

ORIGINAL RESEARCH

Bioaerogels produced from tempo oxidized nano cellulose with chitosan, gelatin, and alginate: general performances for wound dressing application

Orçun Çağlar Kurtuluş · Sedat Ondaral · Nuray Emin · Ali Eslem Kadak

Received: 23 March 2024 / Accepted: 6 November 2024 / Published online: 15 November 2024

Abstract In this study, TEMPO (2,2,6,6 tetramethyl-piperidine-N-oxyl) oxidized nanofibrillated celluloses (CNFs; CNF1 having a higher amount of carboxyl fraction; 1.0613 mmol/g, CNF2 having a lower degree of carboxyl fraction; 0.5543 mmol/g) with different amounts of carboxyl and aldehyde fractions were prepared as the main aerogel matrix, and chitosan (Ch), gelatin (Gl), and alginate (Al) biopolymers were added into suspension with different ratios (100%, 75–25%, 50–50%, 25–75%). Aerogels were produced using a simple freezing and lyophilization procedure, and their suitability for use in wound dressings and other biomedical applications was evaluated. In addition to micro and morphological images, water-PBS (phosphate buffered saline) absorption rates, water vapor permeability (WVP), antibacterial efficacy, and biocompatibility tests were undertaken to study these particular features. The acquired results showed that CNF1-Gl and CNF2-Al based samples had the highest water absorption values (WAV); however, PBS results had the highest values for CNF1-Al 50–50% and CNF2-Al 75–25%, respectively. WVP data were aligned as lines from the highest to lowest degree in CNF1, CNF2, Al, Ch, and Gl. CNF1-Al showed the highest level of WVP data of 4191 g/m^2 day. A microbiological study revealed that CNF/Ch and CNF/Gl bioaerogels had a greater antibacterial impact on both bacterial strains, *S. aureus* and *E. coli*. In contrast, CNF-Al based aerogels showed no antibacterial activity against either strain. The most obvious outcome is that all aerogels are biocompatible, allowing cell development on the material surface. As a result, these aerogels could be used as wound dressings in a variety of biomaterial applications.

Keywords Aerogel · Nanofibrillated cellulose · Chitosan · Gelatin · Alginate

Supplementary Information The online version contains supplementary material available at https://doi.org/10.1007/s10570-024-06282-0.

O. Ç. Kurtuluş (✉)
Department of Material and Materials Processing Technologies, Tosya Vocational School, Kastamonu University, 37300 Kastamonu, Turkey
e-mail: ckurtulus@kastamonu.edu.tr

S. Ondaral
Faculty of Forestry, Department of Forest Products Engineering, Karadeniz Technical University, 61000 Trabzon, Turkey

N. Emin
Faculty of Engineering and Architecture, Department of Biomedical Engineering, Kastamonu University, 37000 Kastamonu, Turkey

A. E. Kadak
Faculty of Fisheries, Department of Aquaculture, Kastamonu University, 37000 Kastamonu, Turkey

Introduction

Aerogels are light weighted, low density, and highly porous materials that were first discovered by Kistler (1932, 1937). The basic production process broadly depends upon the removal of liquid solvent from the gelous phase of the main matrix by different techniques. Lyophilization (freeze drying), supercritical CO_2, and ambient pressure drying have been widely used for this purpose. According to drying technique and the used raw material, porous structured, and light-weight materials are obtained. These materials have been used in a wide range of industrial applications, including dust collectors, catalysts, fuel cell electrodes, heat and sound isolators, dust collectors, and biosensors. These materials' unique qualities include high porosity, high specific surface area, mechanical strength properties, low density, and producibility by using both synthetic and biobased polymers. However, recent investigations about aerogels have mainly focused on biomedical products such as hemostats and wound dressing materials, in addition to drug delivery systems (Kistler 1937; Hrubesh 1998; Guilminot et al. 2007; Olsson et al. 2010; Stergar and Maver 2016; Lovskaya and Menshutina 2020; Liu et al. 2023; Chaudhary et al. 2024; Gorshkova et al. 2024; Sun et al. 2024; Wang et al. 2024; Yue et al. 2024). Biobased polymers such as cellulose, have also shown promise as a raw material for the production of aerogels by dissolving cellulose substances in a variety of solvent systems, including NMMO (N-methyl-morpholine-N-oxide) (Innerlohinger et al. 2006; He et al. 2023; Ma et al. 2023), NaOH-Urea, LiOH-Urea (Cai et al. 2008; Wang et al. 2014; Zhang et al. 2022), LiCl (Litium chloride)-DMAc (Dimethylacetamide) (Duchemin et al. 2010; Garemark et al. 2020). The resulting cellulose substrate was then coagulated, solvent exchanged, and subliminated by supercritical CO_2 drying or lyophilization.

Though it originated in antiquity, the application of conventional gauze and various bandages to wound healing techniques continues to this day (Majno 1975; Jones 2006; Daunton et al. 2012). In the past, the general idea about wound healing was to keep wounds hypothermic until the suggestion by Winter (1962) about closing wounds with a polymeric dressing. After that, new parts of the healing process have emerged, and hydrophilic cotton, gauze, and gauze patches-especially those made of biobased polymeric compounds-have begun to be investigated as potential materials for wound dressings in place of conventional bandages like synthetic ones. As a biobased material with biocompatible and nontoxic properties, CNFs have started to be investigated for application as a wound dressing material in surgical operations. The CNFs are obtained by different mechanical disintegration techniques of the cell walls of wood and agricultural wastes with a high pressure effect by different apparatus called a homogenizer, a microfluidizer, a microgrinder, and a high intensity ultrasonicator. According to the raw material and applied pretreatments (oxidation, sulfonation, acetylation, enzymes, carboxymethylation, etc.) 5–50 nm in width and micron-scaled length fibrils are obtained (Abdul Khalil et al. 2014; Nechyporchuk et al. 2016). The primary benefits of this material include its biobased, biocompatible, and biodegradable nature. These attributes enable its potential applications in a variety of fields, including optical films, composite networks, catalysts, barrier films, papermaking and packaging additives, raw materials for microelectronics and cosmetics, space clothes, fire retardant materials, and viscosity regulator-emulgator in the food, paint, and coating industries. (Henriksson et al. 2008; Mörseburg and Chinga-Carrasco 2009; Belbekhouche et al. 2011; Martins et al. 2012; Sehaqui et al. 2012; Leijonmarck et al. 2013; Martins et al. 2013; Abdul Khalil et al. 2014, Ondaral et al. 2015; Wong et al. 2015; Hassan et al. 2016; Mulyadi et al. 2016; Osong et al. 2016; Xiao et al. 2016; Jiang et al. 2017; Guo et al. 2018; Mao et al. 2019; Li et al. 2020; Qin et al. 2021; Andze et al. 2024; Fernandez Santos et al. 2024; Lin et al. 2024).

As a soluble form of chitin, Ch is an interesting and promising material in many different industries, especially because of its own cationic nature. Structural character is basically composed of β-(1–4) linked 2 amine deoxy β-D- glycopyranose units, and it is the deacetylation product of chitin. The primary significance of this substance lies in its status as a naturally occurring cationic charged polymer, derived from amine groups. Nevertheless, it also possesses favorable characteristics such as being biobased, biodegradable, biocompatible, nontoxic, antimicrobial, bacteriostatic, antioxidant, and antifungal. Ch has been widely used, initially for waste water purification, and has gained importance recently in agriculture, cosmetics, the food industry, textiles, membrane

production, packaging, and biomedical applications (Struszczyk 2002; Hu and Luo 2021; Cazon and Vázquez 2021; Flórez et al. 2022; Gao and Wu 2022; Yang et al. 2022; Jafernik et al. 2023; El-Araby et al. 2024).

The Gl is mostly produced by hydrolyzing collagen protein with acid, alkali, or hot water treatments (Khakalo et al. 2014; Tan et al. 2023; Cao et al. 2024) and typically contains 85–92% protein, 2–4% mineral salts, and 8–12% water, depending on the raw material and production method (Schrieber and Gareis 2007; Palan Abdullah et al. 2018). The primary effective parameters for the final product of material, in addition to pretreatments, are pH, temperature, and extraction (Johnston-Banks 1990; Gomez-Guillen et al. 2015). Two varieties of Gl are produced in industrial grade depending on whether they are pretreated with acids (isoelectric point pH of 8–9) or alkali (isoelectric point pH of 4–5) (Montero et al. 1990; Norland 1990; Gomez-Guillen et al. 2015). Many industries widely utilize Gl due to its distinctive qualities, which include its biobased nature, biodegradability, biocompatibility, reduced antigenic effect compared to collagen, low cost, controlled physical characteristics, ability to produce a variety of products, amphoteric property, and excellent cell compatibility.

The natural exopolysaccharide Al is generally obtained by processing seaweed and the *Pseudomonas* and *Azotobacter* families of bacteria. Its specific qualities, such as structural composition, modification properties, molecular weight, viscoelasticity, and polydispersity, vary depending on the raw material (algae or bacteria). The basic chemical composition consists of two uronic acids: β-D-mannuronic acid and its C5 epimer, β-L-guluronic acid, interconnected by β-(1–4) links. This linear polysaccharide has a highly hydrophilic nature, which allows it to be used for different purposes in different physical forms (Rehm and Moradali 2018; Dey et al. 2019; Saberi Riseh et al. 2022). Al has gradable qualities such being biobased, biocompatible, non-toxic, extremely hydrophilic, and biodegradable, just as the previously mentioned biopolymers. It has been widely employed for many commercial applications as a viscosity regulator, stabilizer, additive, and fertilizer, as well as in a variety of industrial sectors, such as food, textile, cosmetic, pharmaceutical, packaging, and agricultural (Rehm and Moradali 2018; Wang et al. 2023; Zhang et al. 2023; Duong et al. 2024; Elhadef et al. 2024; He et al. 2024; Vaziri et al. 2024).

The literature search yielded results for hydrogel-based products, but it did not turn up any studies on aerogels made of CNF/Ch, CNF/Gl, or CNF/Al. This study's primary goal is to find out how well CNF-biopolymer based aerogels work as wound dressings. CNF/Ch, CNF/Gl, and CNF/Al based aerogels were produced by sequential freezing and lyophilization at varying biopolymer mixing rates. Water-PBS absorption, WVP tests, antibacterial activity, SEM imaging, and biocompatibility tests were performed to assess these composites' suitability for application as biomedical precursors in special wound dressing applications.

Materials and methods

Materials

The magnesium bisulfite pulp used in CNF production was kindly provided by Biocell Paskov a.s. (Czechia). The Ch (deacetylation degree ≥ 75%, viscosity 200–800 cps c: 1% in 1% acetic acid) was purchased from Sigma-Aldrich Chemie GmbH (Taufkirchen, Germany). Gl (100% bovine skin-based, alkalen-pretreated, 83–90% protein, 8–12% water, and the rest salts) was supplied by Yiğitoğlu Chemical Industry (İstanbul/Turkey). The Al (Mw: 1.039.432 g/mol) was kindly provided by Setaş Chemical Inc. (Çerkezköy, Turkey). In addition, TEMPO (2,2,6,6, tetra-methyl-piperidine-N-oxyl), sodium bromide (NaBr), sodium hypochloride (NaClO), sodium hydroxide (NaOH), calcium chloride ($CaCl_2$), magnesium chloride ($MgCl_2.6H_2O$), acetic acid, and ethanol were provided by Sigma-Aldrich Chemie GmbH (Taufkirchen, Germany). PBS solution was prepared by using 0.2 M NaH_2PO_4, KH_2PO_4, and 0.15 M NaCl, all of which were obtained from Merck Millipore (Burlington, Massachusetts, ABD). α-MEM (Euroclone, Italy), fetal bovine serum (FBS) (Sigma, Germany), and penicillin-stereomycin (Sigma, Germany) were used for cell culture studies. MTT ([3-(4,5-dimethylthiazol-2-yl)-2,5 diphenyltetrazolium bromide]) test kit (Sigma, Germany) was used for cytotoxicity studies.

TEMPO oxidation of cellulose

TEMPO oxidation of cellulose was processed according to Saito et al. (2006); 1 g of pulp was dissolved in 100 ml of deionized water with 0.1 mol of TEMPO and 1 mol of NaBr. The pH of the slurry was adjusted to 10, and NaClO (3 mmol/g and 8 mmol/g) prepared at pH 10 was added to the suspension. Suspension was stirred by a mechanical mixer at 500 rpm, and pH was kept stable at 10 by the addition of NaOH. The reaction was stopped by adding 50 ml of ethanol. Fibers were washed with deionized water until drained water conductivity was measured below 5 µS/cm. TEMPO oxidized CNFs (nanofibrillated celluloses) were produced by passing 1% concentrated fiber suspensions through a high-pressure homogenizer (APV 1000, Hemisan/Turkey) at different pressures: 8 mmol TEMPO oxidized cellulose suspension two times at 50–250 bar and 150–550 bar, respectively, while suspension treated with 3 mmol TEMPO was passed at 100–500 bar and 200–800 bar for two times. NC gels were stored at + 4 °C before use.

Production of Ch, Gl, and Al solutions

The Ch solution was prepared by dissolving polymer in deionized water at a concentration of 2%. Acetic acid was added dropwise to the solution until it reached pH 4.9–5. After mixing for 24 h, the solution was filtered and prepared at 1% concentration before use. Gl stock was prepared by dissolving it in deinonized water at 1% concentration at 35–40 °C and used immediately after production. For removing impurities in Al, the polymer was dialyzed before use by means of a membrane cut-off of 12,000 against deionized water. After obtaining conductivity below 5 µS/cm, excess water was removed by using a rotary evaporator, and polymer stock was prepared at 1%.

Aerogel production

The biopolymer solutions (CNFs, Ch, Gl, and Al) were prepared at a 1% concentration at pH 5.5. After adding the calculated amount of Ch into CNF solutions, mixtures having different amounts of CNF and Ch were mixed with a homogenizer (VELP Scientifica, OV 5, Italy) at 10,000 rpm for 5 min; however, CNF/Gl and CNF/Al solutions were mixed by a magnetic stirrer at 300 rpm for 24 h. Following mixing, the gels were transferred into 60 × 15 mm glass petri dishes and cooled to −86 °C before being lyophilized (Christ, Alpha 1–2 LD, Germany) for 48 h at −55 °C and −50 mbar vacuum. Differing from CNF/Ch and CNF/Gl aerogels, due to the very low liquid resistance of Al, CNF/Al based aerogels were crosslinked by soaking in a 100 ml $CaCl_2$ (1%) solution for 12 h even after first obtaining aerogels. After removing excess $CaCl_2$, samples were washed with deinoized water, frozen, and lyophilized again, respectively, under the same conditions.

Water-PBS absorption of aerogels

The water absorption of composites was performed by putting 5 mg of samples into 50 ml of deionized water, which was incubated in an oven at 37 °C for 24 h. PBS absorption tests were also designed as the same procedure as water absorption tests; however, 10 ml of PBS was used as a solution. Samples were placed between paper towels to remove excess liquid, and both water and PBS absorption tests were done in triplicate. Absorption values were calculated by using average values according to Eq. 1:

$$Water - PBS\,Absorption\,Value(\%) = \frac{M_{t-}M_0}{M_0}x100 \quad (1)$$

where M_t and M_0 are sample weights (g) after and before test, respectively.

Water vapor permeability (WVP) of aerogels

WVP tests were performed in triplicate according to ASTM standart (E 96/96M, 2002) with a slight modification. Glass bottles (8.5 cm height; 1.2 cm width) including 6 ml of deionized water were used as templates, and aerogels were adhered to top of the bottles. Apparatus were put into a dessicator, which comprises saturated $MgCl_2.6H_2O$ and provides medium humidity at 40%. The dessicator and samples were kept in an autoclave at 37 °C for 24 h. The weights of the apparatus were measured, and permeability was calculated according to Eq. 2.

$$Water\,Vapor\,Permeability = \frac{(\Delta w/\Delta t)}{A} \quad (2)$$

where Δ_w/Δ_t is humidity lost during 24 h (g/day), and A is a specific humidity transfer area (0.00002826 m^2).

Antibacterial efficiency of aerogels

The antibacterial performances of samples were determined by Zhou et al. (2006) with slight modifications. *Escherichia coli* and *Staphylococcus aureus* bacteria were used for the test, and a three repeat test was performed. Each strain of bacteria was cultured in broth medium at 37 °C for 24 h. Bacterial density was adjusted to approximately 0.7 McFarland by physicological saline solution. Before being measured, samples were cut to almost identical sizes and sanitized for 30 min under a UV light. Composites were put into 24-well culture plates, including 1 ml of medium. After culturing for 24 h at 37 °C, colonies of bacteria were counted according to the method of Miles and Misra (1938).

Biocompatibility of aerogels

Biocompatibility tests of aerogels were performed at Kastamonu University, Central Research Laboratory, Tissue Engineering, Biomaterial and Stem Cell Lab. Unit. Analysis was processed by the MTT [3-(4,5-dimethylthiazol-2-yl)-2,5 diphenyltetrazolium bromide] (Sigma-Aldrich Chemie GmbH (Taufkirchen/Germany)) test based upon cell viability and mitochondrial dehydrogenase activity according to ISO EN 10993-5. Rat bone marrow mesenchymal stem cell lines (MSC) were used in the laboratory cell library. All samples were put into a 24-well plate and prewetted with the culture medium prior to cell seeding. Then, MSC were seeded in each well at a concentration of 1×10^5 cells/well. The culture medium consisted of α-MEM containing 10% FBS, 100 U/ml penicillin, and 100 µg/ml streptomycin. Cell-aerogel constructs were incubated at 37 °C, 5% CO_2, and 95% humidity. Proliferated cells' mitochondrial activity and viability were tested at the end of the 1st, 3rd, and 7th days of culture by MTT based analysis. For this purpose, cell-aerogel constructs were taken at the same dimentions and put into the 96-well plate. Then, fresh medium without PBS (270 µl) was put into each well, and 30 µl of the MTT (5 mg/mL) kit was added to obtain a 10% total concentration. Cultures were incubated at 37 °C, 90% humidity, and 5% CO_2 for 4 h. The formation of formazan crystals was investigated by an inverted phase-contrast microscope (Leica DMIL LED, Germany) at the end of the incubation process. Dark blue formazan crsytals were dissolved in MTT solvent (10% HCl in 2-propanol) and color intensity was measured at 570 nm using a microplate reader (Biotek Synergy-HTX, USA). MTT tests were performed in triplicate for each culture and the average of the measurements was evaluated.

SEM ımages

SEM images of aerogels with high biocompatibility were provided by means of FEI Quanta FEG 250 (USA). Similar weighted and heighted samples were prepared from both surface and cross sections without damaging material and coated with gold–palladium (40 mA current, 50 mbar pressure) by using Cressington Spray Coater (Ted Pella Inc., USA) before measurement.

Results and discussion

Water-PBS absorption

The water absorption performances of aerogels are illustrated in Fig. 1a, b. It can be seen from the figure that all samples show different water absorption values (WAV). The highest amount can be seen for CNF1/Gl 75–25% aerogels as 1584%, and the second highest value is obtained by CNF1/Gl 50–50% based composition. However, the minimum WAV belongs to the CNF1/Ch 25–75% sample. The WAV for CNF2 and biopolymer-containing composites is shown in Fig. 1b, where lower values are attained in comparison to CNF1 aerogels. In contrast to CNF1, CNF2/Al 75–25% had the highest absorption value. However, the minimum values were obtained by CNF2/Ch 25–75%. Overall, it is evident that compared to CNF2 and CNF2/biopolymer based samples, WAV levels were higher in CNF1 and CNF1/biopolymer composites.

Liquid absorption is a critical point of materials used in wound dressing applications, to prevent absorption of wound exudates leaking during the healing process and to ensure that wound sites are cleaned where bacterial infusions reduce the healing rate adversely. According to data on water absorption,

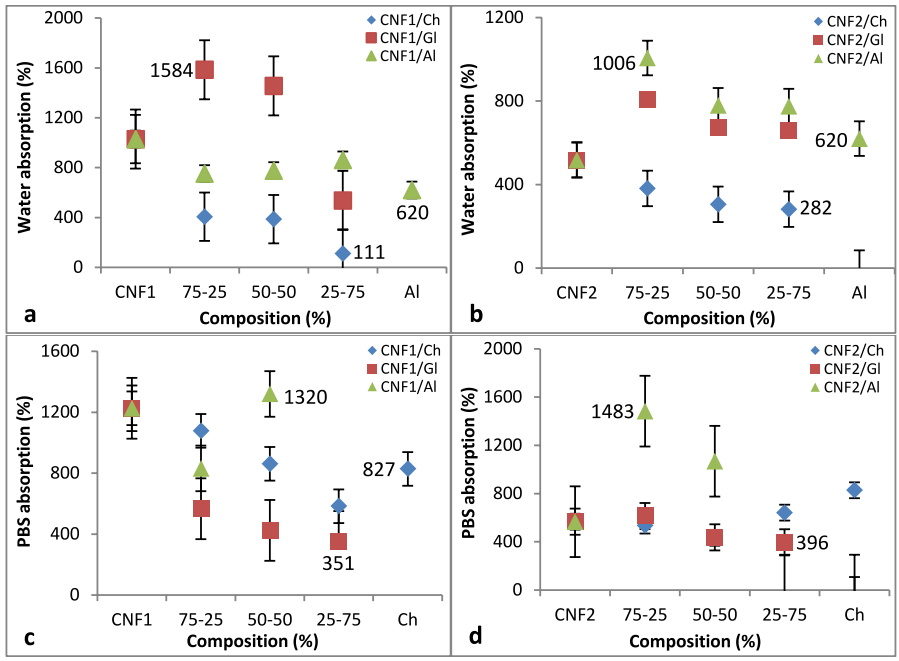

Fig. 1 Water-PBS absorption results of CNF1/biopolymer **a–c** and CNF2/biopolymer **b–d** based aerogels

aerogels based on CNF1/biopolymer often have greater values than mixed composites made of CNF2. The scenario can be explained by the strong hydrophilic chemical moities of CNF1's carboxyl and carbonyl groups. These groups increase interaction with water and components inside aerogels. However, it is also seen that CNF1/Gl samples show a higher rate of WAV due to the highly hydrophilic nature of both CNF and Gl. Low levels of absorption results for CNF1/Ch can be explained by the higher chemical interaction of CNF1's carboxyl groups with Ch's $-NH_2$ groups. It is also clear that increasing amounts of Ch in the composition affect absorption properties adversely. Similar results about absorption properties were proposed by different researchers. Lv et al. (2014) prepared dissolved cellulose-Ch based sponges and stated decreasing water absorption by addition of Ch amount, which was explained by Ch's nondissolving property in water arising out of $-NH_2$ groups. It was also stated that crosslinking between cellulose and Ch caused a compact structure that diminished liquid absorption as a result of shrinking pore sizes. Wu et al. (2014) also performed the water absorption performance of CNF-Ch films and recorded that the absorption rate increased with a higher amount of CNF. The CNF1 and CNF2 matrices' capacity to absorb water reduced as Ch levels rose. Similar trends were observed in CNF/Ch-based samples by Rizal et al. (2021), and this circumstance was attributed to the high concentrations of –OH groups in CNFs in addition to a larger pore size than pure Ch. Similar absorption values were determined for CNF2/biopolymer based aerogels in a recent study. The limited chemical interaction between the low carboxyl fraction of CNF2 and Al, which resulted in the creation of very hydrophilic non-reacted Al molecules, is likely the reason why CNF2/Al based composites were able to determine the highest values. The WAV decreased when Al was added to the CNF matrix; this phenomena can be attributed to the CNF/Al samples' crosslinking in the $CaCl_2$ solution. Ca^{+2} ions also inhibited free carboxyl groups in composites as a result of crosslinking, and polymeric blocks lost their hydrophilic properties.

In Fig. 1c, d the PBS absorption values of aerogels are illustrated. In part c, CNF1/biopolymers' absorption performances are seen, and the highest level was proven by the CNF1/Al based sample composition of 50–50% as 1320%. Both pure Al and 25–75% mixing rated samples' PBS absorption values could not be determined due to the highly hydrophilic nature of Al. The primary mechanism between the composition of Al and CNF1 is explained by the high carboxyl fraction of CNF1 and the carboxyl groups present

in the Al molecule, which probably provide a higher level of absorption with the positive ions in the PBS solution, such as Na^+ and K^+. Figure 1d depicts the PBS absorption values of CNF2/Al based aerogels, with a clearly evident increased level of absorption. Even though porosity, surface area, and pore diameter values were comparable, this condition was probably made better by the higher pore volume of CNF2/Al based aerogels. Examining the PBS absorption degrees of the CNF1/Ch samples, it was found that the absorption values decreased when Ch was added to the CNF1 matrix. This behavior of Ch was studied by Ondaral et al. (2018), in which PBS absorption behaviors of films produced by mixing CNFs having different amounts of aldehyde fractions with Ch were studied by using quart crystal microbalance (QCM-D). According to the results, the addition of Ch to CNF affected PBS absorption negatively compared to pure CNF based films. This situation was explained by blocking functional groups of CNFs by Ch. Compared to film structure, aerogels are highly porous materials, and a higher level of liquid absorption in this study is almost expected. In general, PBS absorption performances of CNF2/Ch based aerogels were found to be poorer than those of CNF1/Ch based ones. The reduced degree of carboxylic fraction in CNF2 provides a clear explanation for this phenomenon. Low amount carboxyl groups interacted in a lower degree with cationic salts of PBS solution. In addition, Ch's cationic charges can be responsible for decreasing absorption values, and positive charges probably repel cationic ions in PBS. In addition to Ch and Al based aerogels, PBS absorption values for CNF/Gl based samples can be observed in the same figure, with a clear decreasing trend with Gl addition to the composition. A small difference was found when comparing CNF1/Gl and CNF2/Gl aerogels, and the tendency with Gl addition is most likely due to Gl's very hydrophilic character, which is comparable to Al.

WVP of aerogels

In Fig. 2, the WVP results of all aerogels are given. When compared to CNF/Ch based samples, all aerogels showed similar WVP results, with values ranging between 3297 and 3011 g/m^2 day. The CNF/Gl composites have the lowest WVP results among all samples, ranging between 2367 and 2091 g/m^2 day. CNF1/Al aerogels have a higher value of WVP than CNF2 mixed samples. The highest value of all the aerogels is 4191 g/m^2 day, which is the maximum WVP findings found for the composite of CNF1/Al 75–25%.

Pure CNF based aerogels have similar WVP amounts of 3297 g/m^2 day and 3167 g/m^2 day for CNF1-2, respectively. Pure biopolymeric aerogels had values of about 2700–3000 g/m^2 day, and these quantities were almost lower when compared to both pure CNFs and compositions with polymers. In general, CNF/Ch mixed samples show higher values compared to neat ones. A similar result was obtained by Shieh et al. (1998) by comparing the higher sensibility of Ch's -NH_2 groups presented in a higher amount in structure than CNF's -OH molecules against water molecules. Higher Gl amounts in composition caused a decrease in WVP results, especially for CNF1/Gl, which was also indicated by Taokaew et al. (2013). They found that WVP values decreased for bacterial cellulose (BC)-Gl composites by increasing density with a higher amount of polymer in the composition. However, the highest WVP results belong to CNF1/Al 75–25% samples, and this situation is thought to be a result of the higher pore diameter of these

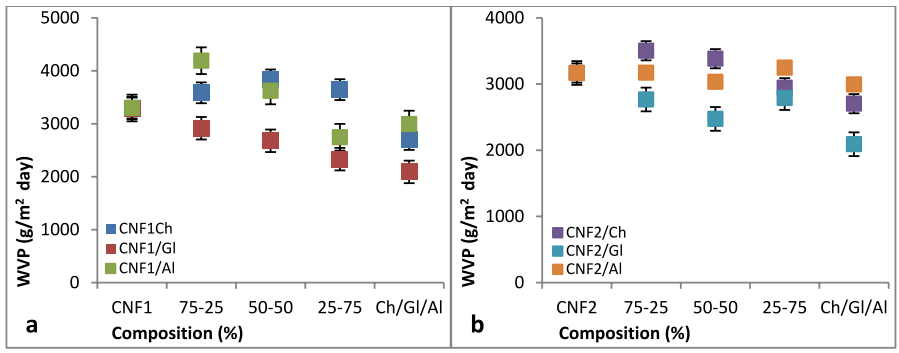

Fig. 2 WVP results of CNF1/biopolymer **a** and CNF2/biopolymer **b** based aerogels

materials, which was determined as 3.10 nm as given in Table 1 according to our previous work (Kurtuluş et al. 2023).

The figure clearly shows that aerogels based on CNF1/Al have a higher degree of WVP than aerogels based on CNF2. On the other hand, a declining trend is also seen when the amount of Al increases. As porosity levels essentially determine WVP, our earlier research (Table 1) indicates that aerogels based on CNF1/Al had higher porosity, surface area, pore volume, and diameter values than samples based on CNF2/Al. In addition, CNF2/Al 25–75% mixing rated composites' WVP results show a higher degree than CNF1/Al 25–75% based composites. The higher specific surface area and relative pore volume of CNF2/Al 25–75% are responsible for this result, which can be seen in Table 1. Huq et al. (2012) proposed decreasing the trend of WVP by adding nanocrystalline cellulose (CNC) to the Al matrix. This situation was explained by the formation of tangles by CNC in the skeleton that diminished the diffusion process. When compared to CNC, CNF has amorphous regions that provide higher diffusion rates, which can be explained by its high porosity values. Wang et al. (2017) prepared films with CNC and cellulose fibril with Al and reported that CNC-Al composites' WVP values were lower than cellulose fibril-Al based ones. This circumstance was explained by the fact that cellulose fibrils are significantly more hydrophilic than CNCs. According to results, CNF aerogels as a porous material can be used in wound dressing applications by being processed at the optimum WVP rate, which is essential for different types of dressers. Normal skin's WVP rate is 204 g/m^2 day; however, this value is 279 g/m^2 day for first-degree burn wounds and 5138 g/m^2 day for granulation tissues. In current research, all aerogels have appropriate values for being used in related dressing applications (Lin et al. 2013; Lv et al. 2014).

Table 1 Surface area, pore volume and pore diameter values of aerogels

Sample	Surface area (m^2/g)	Pore volume (cm^3/g)	Pore diameter (nm)
CNF1	329	0.308	3.12
CNF2	299	0.220	3.30
CH	355	0.357	3.29
GL	357	0.319	2.97
AL	330	0.310	3.12
CNF1/CH 75–25	176	0.159	2.96
CNF1/CH 50–50	226	0.202	3.30
CNF1/CH 25–75	174	0.162	2.96
CNF2/CH 75–25	247	0.208	3.28
CNF2/CH 50–50	221	0.200	3.11
CNF2/CH 25–75	139	0.122	3.46
CNF1/GL 75–25	415	0.377	3.14
CNF1/GL 50–50	382	0.345	3.13
CNF1/GL 25–75	305	0.264	3.12
CNF2/GL 75–25	332	0.298	3.12
CNF2/GL 50–50	318	0.193	3.12
CNF2/GL 25–75	390	0.346	2.97
CNF1/AL 75–25	310	0.281	3.10
CNF1/AL 50–50	300	0.264	3.10
CNF1/AL 25–75	272	0.235	3.01
CNF2/AL 75–25	318	0.306	3.10
CNF2/AL 50–50	313	0.301	3.00
CNF2/AL 25–75	300	0.265	3.09

Antibacterial efficiency of aerogels

Antibacterial efficiencies were performed with gram positive (*Staphylococcus aureus*) and gram negative (*Escherichia coli*) bacteria strains. According to the method, 0.7 McFarland colonies were used as the starting medium, and the inhibiton characteristics of bacteria on aerogel samples after 24 h were calculated, and the results are given in Table 2.

All CNF/Ch based aerogels and neat CNF based samples showed antibacterial effects by reducing bacteria colony amounts or inhibiting colony growth at any and every mixing ratio. The maximum antibacterial effect for gram positive bacteria was observed by NC2/Ch 25–75% aerogel, which reduced the starting colony amount from 2×10^9 used in the test to 1×10^5 for *S. aureus*. Table 2 also shows the antibacterial efficiency versus the gram negative bacteria *Escherichia coli*, and similarly, all samples showed the inhibiting efficiency proposed by 25–75% mixing rated sample on the 10^3 scale. Antibacterial activity for both bacteria strains was also provided by CNF/Gl samples. Pure polymer based aerogels show bacteria counts of 10×10^6 and 7×10^7 for CNF1 and CNF2, respectively, which was a lower amount of bacteria used during the test, 2×10^9. Neat Gl based aerogels' bacterial resistance could not be determined due to decomposition in the PBS solution for both strains.

Table 2 Antibacterial efficiency of aerogels versus *Staphylococcus aureus* and *Escherichia coli*

	S. aureus						*E. coli*		
Sample	10^4	10^5	10^6	10^7	10^8	10^9	10^3	10^5	10^6
CNF1			10					84	
CNF2				7					42
Ch	x	x					140		
Gl									
Al						x			
CNF1/Ch 75–25				0				144	
CNF1/Ch 50–50		7							40
CNF1/Ch 25–75			18						1
CNF2/Ch 75–25			1						140
CNF2/Ch 50–50		7							112
CNF2/Ch 25–75		1							2
CNF1/Gl 75–25				1					
CNF1/Gl 50–50				0					
CNF1/Gl 25–75				1					
CNF2/Gl 75–25				0					
CNF2/Gl 50–50				0					
CNF2/Gl 25–75					34				
CNF1/Al 75–25						66			
CNF1/Al 50–50						150			
CNF1/Al 25–75						0			
CNF2/Al 75–25						76			
CNF2/Al 50–50						0			
CNF2/Al 25–75						12			

The maximum effect of composites was generally provided by CNF1/Gl composites with a mixing rate of 75–25% as 1×10^7 and 25–75% as 1×10^7. However, the minimum effect was provided by CNF2/Gl at 25–75% for a 34×10^8 bacteria count. CNF/Gl composites also have an antibacterial effect against *Escherichia coli*. Pure CNF samples' bacteria colonies on the surface were determined to be 84×10^5 and 42×10^6 for CNF1 and CNF2. Additionally, CNF/Al based aerogels are not resistant to both bacterial cultures. The starting amount of used bacteria (2×10^9) for the test increased to a generally determined range of nearly 10^9.

Bacterial invasion of the wounded area is an adverse situation because it delays the wound healing process by infecting related areas. For this reason, antibacterial activity is a fundamental property of wound dressing materials. The table makes it evident that all CNF/Ch based aerogels have antibacterial activity against the two types of bacteria. The pure Ch samples showed no inhibition for gram positive bacteria, while a critical decrease in colony amount was observed for gram negative bacteria. This is attributed to Ch's high antibacterial efficiency against *E. coli* by Wu et al. (2016). In addition, samples also showed a much smaller amount of gram negative bacteria than gram positive bacteria, which is confirmed by this definition. Ch and its derivatives have antibacterial efficiency against various kinds of bacteria, as is known. This specification was explained by different workers with such topics as: the polycationic nature of polymers interacts with the negative charge of the bacteria cell wall and inhibits the growth of bacteria; high concentrations of Ch provide accumulation on bacteria and prevent activity; and also the retention of Ch on the DNA of bacteria and prevent progressing mRNA (Lin et al. 2013; Cao et al. 2016). Another important piece of data seen in the table is the antibacterial effect of pure CNF samples. This result also shows correspondence with a study proposed by Rees et al. (2015). Similar antibacterial effects from different studies also showed parallel results with this

study. Cao et al. (2016) produced regenerated cellulose-Ch based membranes for wound healing. They found that all membranes had antibacterial effects against *S. aureus* and *E. coli*. Another promotional study related to antibacterial activity results was proposed by Powell et al. (2016), in which TEMPO oxidized CNF based films were produced, and these films showed antibacterial effects against *Pseudomonas aeruginosa*, which causes infection and delays wound healing. CNF/Gl composites also showed resistance to both bacterial strains. When investigated for gram positive *S. aureus*, all samples showed bacterial resistance, in which pure CNFs had higher resistance compared to NC/Gl aerogels and the maximum efficiency proposed by CNF1/Gl 75–25% and 25–75% based aerogels. However, all samples also had bacterial resistance against gram negative *E. coli*. Similar to gram positive bacteria, the highest bacterial resistance versus gram negative bacteria was also proposed by CNF1/Gl 75–25% composites. In fact, there is no information about Gl's antibacterial efficiency due to the highly dissolving effect of composites in PBS solution in a short time, whereas NC-Gl composites showed bacterial resistance, according to some workers. Islam et al. (2014) produced jute based NC-Gl composites with the addition of CNC to the composition. Results showed that a higher antibacterial effect was achieved by adding 8% CNC into the mixture against *E. coli*. As a result, CNF/Gl aerogels have an antibacterial effect which, showed higher efficiency with the addition of a higher level of CNF in the composition. Contrary to CNF/Ch and CNF/Gl composites, CNF/Al based samples did not show any positive effect against both bacterial strains. All mixing ratios between CNF and Al resulted in a higher amount of bacteria colony on samples than the starting bacteria for the test (2×10^9). The main objectives of Al based wound dressing materials are to absorb wound exudate and form a gelous phase on the wound site. This gel keeps moisture around the wound area and diminishes bacterial contamination, resulting in an increased healing rate (Aderibigbe and Buyana 2018). Al based wound dressing materials were investigated by different researchers, and the general prospect is that Al materials show antibacterial efficiency against different kinds of bacteria. Straccia et al. (2015) used sodium-Al based hydrogels coated with Ch as wound dressing material and proposed that hydrogels had an antibacterial effect against *E. coli*. Hegge et al. (2011) produced curcumin added Al foams and used them for healing infected wounds. According to the results, the addition of curcumin increased the hydration time of foams, and *E. coli* bacteria were affected to a lower degree than *E. faecalis* from curcumin added foams. In addition, it is proposed that with the addition of antibacterial compounds to compositions such as Ag and $AgNO_3$, antibacterial effects could be increased in these composites. Aerogels do not appear to have an antibacterial impact, according to recent research; nonetheless, bacterial colonization was limited to a very low level, preventing bacteria from multiplying more widely on composites. This negative result is probably caused by the pre-dialysis of Al polymer before use in aerogel production, in which low-weight chemical compounds were probably removed. However, these aerogels are being thought of as applicable for wound dressing applications, especially for non-infected wounds.

Biocompatibility of aerogels

The first essential and needed feature of wound dressing materials is biocompatibility, and which is described as the compatibility of related materials with the application area and the tissues near this section without decomposing structure or having toxic properties. In Fig. 3, the biocompatibility results of the CNF1/Ch and CNF2/Ch in addition to pure samples are shown. According to the results, all aerogels have biocompatible properties, and it is clear that increasing amounts of Ch in their composition cause higher cell proliferation rates. Proliferating cell numbers in higher grades grew when Ch was added to the mixing media as opposed to plain CNF precursors. The highest CNF1/Ch performance was found when there was a high percentage of Ch in the CNF matrix, between 25 and 75%, demonstrating how strongly compatible Ch is structurally. The mixing rated sample with a 75–25% ratio had the greatest efficiency in CNF2/Ch samples. The large specific surface area and relative pore volume of the linked aerogels in comparison to other CNF/Ch samples is most likely the source of this scenario. Increasing surface area values usually creates the ideal conditions for cell proliferation by promoting cell movements. One positive outcome is the CNFs' biocompatibility, which opens new doors for employing pure CNFs (CNF1 and CNF2) in the

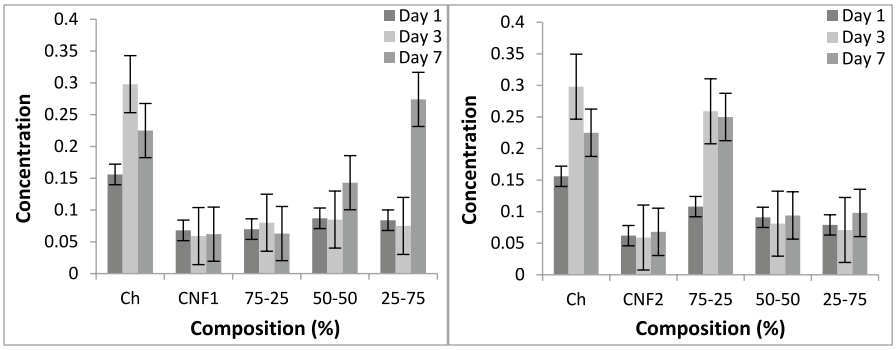

Fig. 3 Cell based biocompatibility results of CNF1/Ch and CNF2/Ch based aerogels

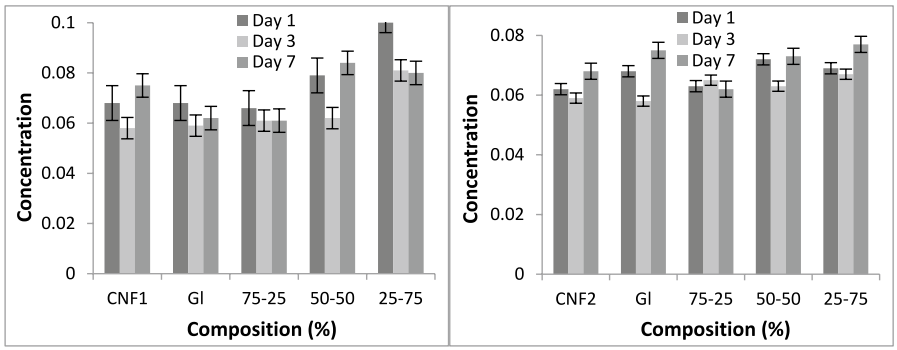

Fig. 4 Cell based biocompatibility results of CNF1/Gl and CNF2/Gl based aerogels

medical business without the need for biopolymer addition. However, Wang et al. (2017) and Fan et al. (2020) also found biocompatibility results for NC–Ch composites that were comparable to our findings.

CNF/Gl composite-related results are shown in Fig. 4, which shows a biocompatible character with different cell amounts on samples. Generally, pure CNFs and Gl samples have similar cell growth values; however, increasing the amount of Gl in the composition provided a higher amount of inhibited-proliferated cells on the samples, especially for 50–50% and 25–75% compositions. In the literature, generally BC based materials were investigated for medical applications, widely compared to CNFs and CNCs. Taokaew et al. (2013) reported a non-cytotoxical effect for both BC and BC-Gl films. In addition, Cai and Kim (2010) also reported similar biocompatibility results for the same composition of films. Researchers submitted that BC-Gl films show higher cell amounts versus pure BC hydrogels. Pei et al. (2015) conducted a study on the biocompatibility of regenerated cellulose-Gl composites, and they also obtained similar outcomes. As the mixing rate was increased, these composites exhibited biocompatibility with increasing Gl percentages.

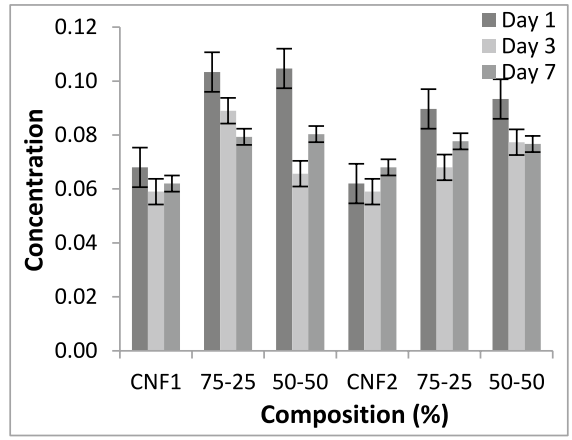

Fig. 5 Cell based biocompatibility results of CNF1/Al and CNF2/Al based aerogels

In Fig. 5, CNF/Al composites' biocompatibility results are illustrated. Different proportioned samples had a biocompatible nature associated with pure aerogels. Crosslinkers were not used to provide mechanical stability for Al based aerogels. That's why pure

Al and 25–75% (CNF-Al) mixing rated aerogels' performances could not be determined due to the highly decomposed samples in the aquagenic solution during examination. When examined for CNF/Al, it is obviously seen that a higher amount of Al in the CNF matrix increases cell adhesion and results in higher degree of proliferation compared to a neat CNF sample. It is evident that the presence of Al in composites improved both biocompatibility and cell survival. This outcome provides details regarding pure Al's biocompatibility. When compared to CNF fractions, there is a minor enhancement of high carboxyl and aldehyde fractionated CNF1/Al aerogels compared to CNF2/Al composites. This situation is probably correlated with high specific surface area and porosity values, which promote higher efficiency of cell bonding into the matrix and result in higher proliferation. CNF1/Al composites have higher porosity values, whereas surface area values (Table 1) are almost similar for CNF1/Al and CNF2/Al composites. According to this view, a small difference between porosity values can have a positive effect on cell viability. In addition, degradation in PBS solution during biocompatibility tests can be another effect of aerogels' performances. Maintaining structural integrity during performance can have a positive effect on cells moving between interconnected pores and result in higher values of adhesion and proliferation in the aerogel network. In summary, one of the most important requirements for tissue scaffolds and useable materials in these applications is shared by all CNF/biopolymers.

SEM ımages

Figure 6 a–d shows macro surface cross sections of CNF1/Ch 25–75% and CNF2/Ch 75–25% based aerogels, both of which have high biocompatibility rates. For CNF1/Ch 25–75%, the macro structure topography is visible clearly and uniformly with a white-yellowish color, but the sample sides are oriented toward the interior of the region, which is primarily the result of a strong vacuum effect during lyophilization that caused Ch fibers to migrate to the surface from the interior of the matrix. The microsurface's network of connected cell walls is particularly responsible for its high porosity structure. Conversely, a cross section reveals closed, thick layers that are also visible in macro cross pictures. This closely spaced area may have been formed by Ch clumping together during the freezing process. Figure 6c–d displays the macro and SEM views of the CNF2/Ch 75–25% mixing rated aerogel. Images of a homogeneous macro surface exhibit an almost white color without complication. This situation is further supported by surface SEM pictures, which show strongly directed and linked cells. However, the supplied sample from the entire composite structure clearly reveals a two-layered

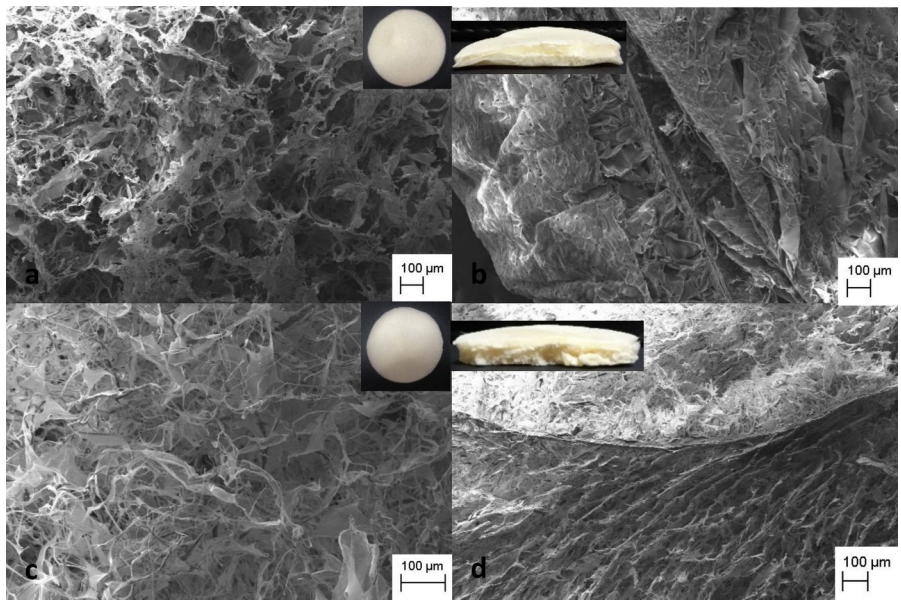

Fig. 6 SEM Images of aerogels **a**, **b** CNF1/Ch 25–75% surface and cross section, **c**, **d** CNF2/Ch 75–25% surface and cross section

cross section, which was previously interpreted as a Ch fiber aggregation via the drying line.

Conclusion

In current research, CNFs with different amounts of carboxyl and aldehyde fractions were produced by sequential pretreatment of TEMPO oxidation and homogenization processes. Biopolymers of Ch, Gl, and Al were prepared at 1% concentration at pH 5.5 and added into the CNF matrix in proportions of 75–25%, 50–50% and 25–75%. Cylindirical, homogenous aerogels were produced to investigate the efficiency of related materials for wound dressing or not. Water-PBS absorption rates, WVP tests, antibacterial efficiency, and bicocompatibility performances were also investigated with SEM images. The findings show that all aerogels, with the exception of pure Ch and Gl based aerogels, which are classified as extremely hydrophilic polymers, have sufficient water-PBS absorption rates. WVP tests also showed all samples, both pure CNFs and those combined with biopolymers, had a high amount of evaporation rate for different types of wounds. In order to inhibit bacterial invasion which lead to infection of wound area and therefore prolongs needed healing time, generally it is desired to be antibacterial effect of materials being used as a wound dressing. This specification was performed for both gram positive and gram negative bacteria strains. Related results showed that CNF/Ch and CNF/Gl composites have a high antibacterial effect, although CNF/Al compositions showed no antibacterial effect against two bacteria strains, and they were proposed to be used for non-infectious wounds. Biocompatibility tests were performed to determine cell viability, and all aerogels were found to be biocompatible, which is the most important parameter for materials to be usable as tissue scaffold materials. When the obtained results were qualified, the main idea was that the produced composites fulfilled specific features required for scaffold materials and were also usable precursors in these applications after in vivo tests.

Acknowledgments The authors kindly acknowledge SETAŞ Chemical Inc. and YİĞİTOĞLU Chemical Group for supplying gelatin and alginate polymers, respectively during all study.

Author contribution Orçun Çağlar KURTULUŞ: Conceptualization, Methodology, Investigation, Writing—Original Draft, Visualization. Sedat ONDARAL: Conceptualization, Methodology, Writing—Review & Editing. Nuray EMİN: Methodology, Investigation. Ali Eslem Kadak: Methodology, Investigation.

Funding This research did not receive any specific grants from funding agencies in the public, commercial, or not-for-profit sectors.

Data availability The current study did not produce or analyze any datasets.

Declarations

Conflict of interest The authors declare no competing interests.

References

Abdul Khalil HPS, Davoudpour Y, Nazrul Islam Md, Mustapha A, Sudesh K, Dungani R, Jawaid M (2014) Production and modification of nanofibrillated cellulose using various mechanical processes: a review. Carbohydr Polym 99:649–665. https://doi.org/10.1016/j.carbpol.2013.08.069

Aderibigbe BA, Buyana B (2018) Alginate in wound dressings. Pharmaceutics 10(2):42. https://doi.org/10.3390/pharmaceutics10020042

Andze L, Skute M, Zoldners J, Andzs M, Sirmulis G, Irbe I et al (2024) Enhancing paper packaging's wet strength using the synergy between chitosan and nanofibrillated cellulose additives. Polymers 16(2):227. https://doi.org/10.3390/polym16020227

ASTM E 96/96 M (2002) Standard test methods for water vapor transmission of materials, ASTM International.

Belbekhouche S, Bras J, Siqueira G, Chappey C, Lebrun L, Bertine K, Marais S, Dufresne A (2011) Water sorption behavior and gas barrier properties of cellulose whiskers and microfibrils films. Carbohydr Polym 83(4):1740–1748

Cai Z, Kim J (2010) Bacterial cellulose/Poly(ethylene glycol) composite: characterization and first evaluation of biocompatibility. Cellulose 17(1):83–91. https://doi.org/10.1007/s10570-009-9362-5

Cai J, Kimura S, Wada M, Kuga S, Zhang L (2008) Cellulose aerogels from alkali hydroxide-urea solution. Chemsuschem 1:149–154. https://doi.org/10.1002/cssc.200700039

Cao H, Wang J, Hao Z, Zhao D (2024) Gelatin-based biomaterials and gelatin as an additive for chronic wound repair. Front Pharmacol 15:1398939. https://doi.org/10.3389/fphar.2024.1398939

Cao Z, Luo X, Zhang H, Fu Z, Shen Z, Cai N, Xue Y, Yu YA (2016) Facile and green strategy for the preparation of porous chitosan-coated cellulose composite membranes for potential applications as wound dressing. Cellulose 23:1349–1361. https://doi.org/10.1007/s10570-016-0860-y

Chaudhary S, Dora DTK, Reddy DS, Porwal SK (2024) Sustainable non-cytotoxic ultra-light aerogel derived from waste tissue paper as an effective hemostatic agent. Biomass Convers Biorefinery 14(8):9333–9344. https://doi.org/10.1007/s13399-022-02803-8

Cazon P, Vázquez M (2021) Bacterial cellulose as a biodegradable food packaging material: a review. Food Hydrocoll 113:106530. https://doi.org/10.1016/j.foodhyd.2020.106530

Daunton C, Kothari S, Smith L, Steele D (2012) A history of materials and practices for wound management. Wound Pract Res 20(4)

Dey P, Ramanujam R, Venkatesan G, Nagarathnam R (2019) Sodium alginate potentiates antioxidant defense and PR proteins against early blight disease caused by Alternaria solani in Solanum lycopersicum Linn. PLoS ONE 14:e0223216. https://doi.org/10.1371/journal.pone.0223216

Duchemin BJC, Staiger MP, Tucker N, Newman RH (2010) Aerocellulose based on all-cellulose composites. J Appl Polym Sci 115:216–221. https://doi.org/10.1002/app.31111

Duong T, Vivero-Lopez M, Ardao I, Alvarez-Lorenzo C, Forgács A, Kalmár J, García-González CA (2024) Alginate aerogels by spray gelation for enhanced pulmonary delivery and solubilization of beclomethasone dipropionate. Chem Eng J. https://doi.org/10.1016/j.cej.2024.149849

El-Araby A, Janati W, Ullah R, Ercisli S, Errachidi F (2024) Chitosan, chitosan derivatives, and chitosan-based nanocomposites: eco-friendly materials for advanced applications (a review). Front Chem 11:1327426. https://doi.org/10.3389/fchem.2023.1327426

Elhadef K, Chaari M, Akermi S, Ennouri K, Hlima HB, Fourati M et al (2024) Gelatin-sodium alginate packaging film with date pits extract: an eco-friendly packaging for extending raw minced beef shelf life. Meat Sci 207:109371. https://doi.org/10.1016/j.meatsci.2023.109371

Fernández-Santos J, Valls C, Cusola O, Roncero MB (2024) Periodate oxidation of nanofibrillated cellulose films for active packaging applications. Int J Biol Macromol 267:131553. https://doi.org/10.1016/j.ijbiomac.2024.131553

Fan X, Li Y, Li X, Wu Y, Tang K, Liu J, Zheng X, Wan G (2020) Injectable antibacterial cellulose nanofiber/chitosan aerogel with rapid shape recovery for noncompressible hemorrhage. Int J Biol Macromol 154:1185–1193. https://doi.org/10.1016/j.ijbiomac.2019.10.273

Flórez M, Guerra-Rodríguez E, Cazón P, Vázquez M (2022) Chitosan for food packaging: recent advances in active and intelligent films. Food Hydrocoll 124:107328. https://doi.org/10.1016/j.foodhyd.2021.107328

Gao Y, Wu Y (2022) Recent advances of chitosan-based nanoparticles for biomedical and biotechnological applications. Int J Biol Macromol 203:379–388. https://doi.org/10.1016/j.ijbiomac.2022.01.162

Garemark J, Yang X, Sheng X, Cheung O, Sun L, Berglund LA, Li Y (2020) Top-down approach making anisotropic cellulose aerogels as universal substrates for multifunctionalization. ACS Nano 14(6):7111–7120. https://doi.org/10.1021/acsnano.0c01888

Gomez-Guillen MC, Gimenez B, Lopez-Caballero ME (2015) Functional and bioactive properties of collagen and gelatin from alternative sources: a review. Food Hydrocoll 25(8):1813–1827. https://doi.org/10.1016/j.foodhyd.2011.02.007

Gorshkova NA, Brovko OS, Palamarchuk IA, Ivahnov AD, Bogdanovich NI, Vorob'eva TY (2024) Preparation of an antibacterial composite aerogel for biomedical purposes based on an alginate–chitosan complex and calcium carbonate. Appl Biochem Microbiol 60(2):194–200. https://doi.org/10.1134/S0003683824020042

Guilminot E, Fischer F, Chatenet M, Rigacci A, Berthon-Fabry S, Achard P, Chainet EJ (2007) Use of cellulose-based carbon aerogels as catalyst support for PEM fuel cell electrodes: electrochemial characterization. J Power Sources 166(1):104–111. https://doi.org/10.1016/j.jpowsour.2006.12.084

Guo L, Chen Z, Lyu S, Fu F, Wang S (2018) Highly flexible cross-linked cellulose nanofibril sponge-like aerogels with improved mechanical property and enhanced flame retardancy. Carbohydr Polym 179:333–340. https://doi.org/10.1016/j.carbpol.2017.09.084

Hassan EA, Hassan ML, Abou-Zeid RE, El-Wakil NA (2016) Novel nanofibrillated cellulose/chitosan nanoparticles nanocomposites films and their use for paper coating. Ind Crops Prod 93:219–226. https://doi.org/10.1016/j.indcrop.2015.12.006

He J, Yang S, Goksen G, Cong X, Khan MR, Zhang W (2024) Functionalized pectin/alginate food packaging films based on metal-phenol networks. Food Biosci 58:103635. https://doi.org/10.1016/j.fbio.2024.10363

He S, Li J, Cao X, Xie F, Yang H, Wang C et al (2023) Regenerated cellulose/chitosan composite aerogel with highly efficient adsorption for anionic dyes. Int J Biol Macromol 244:125067. https://doi.org/10.1016/j.ijbiomac.2023.125067

Hegge AB, Andersen T, Melvik JE, Bruzell E, Kristensen S, Tonnesen HH (2011) Formulation and bacterial phototoxicity of curcumin loaded alginate foams for wound treatment applications: studies on curcumin and curcuminoides XLII. J Pharm Sci 100(1):174–185. https://doi.org/10.1002/jps.22263

Henriksson M, Berglund LA, Isaksson P, Lindstrom T, Nishino T (2008) Cellulose nanopaper structures of high toughness. Biomacromol 9(6):1579–1585. https://doi.org/10.1021/bm800038n

Hrubesh LW (1998) Aerogel applications. J Non Cryst Solids 225:335–342. https://doi.org/10.1016/S0022-3093(98)00135-5

Hu Q, Luo Y (2021) Chitosan-based nanocarriers for encapsulation and delivery of curcumin: a review. Int J Biol Macromol 179:125–135. https://doi.org/10.1016/j.ijbiomac.2021.02.216

Huq T, Salmieri S, Khan A, Khan RA, Le Tien C, Riedl B, Fraschini C, Bouchard J, Uribe-Calderon J, Kamal MR, Lacroix M (2012) Nanocrystalline cellulose (NCC) reinforced alginate based biodegradable nanocomposite film. Carbohydr Polym 90(4):1757–1763. https://doi.org/10.1016/j.carbpol.2012.07.065

Innerlohinger J, Weber KH, Kraft G (2006) Aerocellulose: aerogels and aerogel-like materials made from cellulose. Macromol Symp 244:126–135. https://doi.org/10.1002/masy.200651212

Islam MS, Rahman MM, Gafur MA, Mustafa AI, Khan MA (2014) Preparation and characterization of cellulose-gelatin nanocomposite isolated from jute for biomedical application. Mater Sci Indian J 11:105–112

Jafernik K, Ładniak A, Blicharska E, Czarnek K, Ekiert H, Wiącek AE, Szopa A (2023) Chitosan-based nanoparticles as effective drug delivery systems-a review. Molecules 28(4):1963. https://doi.org/10.3390/molecules28041963

Jiang F, Dinh DM, Hsieh YL (2017) Adsorption and desorption of cationic malachite green dye on cellulose nanofibril aerogels. Carbohydr Polym 173:286–294. https://doi.org/10.1016/j.carbpol.2017.05.097

Johnston-Banks FA (1990) Gelatine. In: Harris P (ed) Food gels. Elsevier Applied Science Publisher, London, pp 233–289

Jones VJ (2006) The use of gauze: will it ever change? Int Wound J 3(2):79–88

Khakalo A, Filpponen I, Johansson LS, Vishtal A, Lokanathan AR, Rojas OJ, Laine J (2014) Using gelatin protein to facilitate paper thermoformability. React Funct Polym 85:175–184. https://doi.org/10.1016/j.reactfunctpolym.2014.09.024

Kistler SS (1932) Coherent expanded-aerogels. J Phys Chem 36(1):52–64. https://doi.org/10.1021/j150331a003

Kistler SS (1937) United States Patent No: 2,093,454, Method of producing aerogels.

Kurtuluş OÇ, Ondaral S, Emin N, Aşıkuzun E (2023) Different amount of carboxyl-aldehyde fractionated nanofibril cellulose and main characteristics of chitosan, gelatin, alginate added composites. Int J Biol Macromol 242(2):124824. https://doi.org/10.1016/j.ijbiomac.2023.124824

Leijonmarck S, Cornell A, Lindbergh G, Wågberg L (2013) Single-paper flexible Li-ion battery cells through a paper-making process based on nano-fibrillated cellulose. J Mater Chem A Mater 1(15):4671–4677. https://doi.org/10.1039/C3TA01532G

Lovskaya D, Menshutina N (2020) Alginate-based aerogel particles as drug delivery systems: Investigation of the supercritical adsorption and in vitro evaluations. Materials 13(2):329. https://doi.org/10.3390/ma13020329

Li Y, Jia P, Xu J, Wu Y, Jiang H, Li Z (2020) The aminosilane functionalization of cellulose nanofibrils and the mechanical and CO_2 adsorption characteristics of their aerogel. Ind Eng Chem Res 59(7):2874–2882. https://doi.org/10.1021/acs.iecr.9b04253

Lin WC, Lien CC, Yeh HJ, Yu CM, Hsu SH (2013) Bacterial cellulose and bacterial cellulose-chitosan membranes for wound dressing applications. Carbohydr Polym 94(1):603–611. https://doi.org/10.1016/j.carbpol.2013.01.076

Lin H, Kehinde O, Lin C, Fei M, Li R, Zhang X et al (2024) Mechanically strong micro-nano fibrillated cellulose paper with improved barrier and water-resistant properties for replacing plastic. Int J Biol Macromol. https://doi.org/10.1016/j.ijbiomac.2024.130102

Liu C, Liu C, Shi Z, Yu D, Wang X, Liu S et al (2023) A peptide-engineered alginate aerogel with synergistic blood-absorbing and platelet-binding capabilities to rapidly stop bleeding. Carbohydr Polym 321:121254. https://doi.org/10.1016/j.carbpol.2023.121254

Lv F, Wang C, Zhu P, Zhang C (2014) Characterization of chitosan microparticles reinforced cellulose biocomposite sponges regenerated from ionic liquid. Cellulose 21:4405–4418. https://doi.org/10.1007/s10570-014-0440-y

Ma X, Zhou S, Li J, Xie F, Yang H, Wang C et al (2023) Natural microfibrils/regenerated cellulose-based carbon aerogel for highly efficient oil/water separation. J Hazard Mater 454:131397. https://doi.org/10.1016/j.jhazmat.2023.131397

Mao J, Tang Y, Zhao R, Zhou Y, Wang Z (2019) Preparation of nanofibrillated cellulose and application in reinforced PLA/starch nanocomposite film. J Polym Environ 27:728–738. https://doi.org/10.1007/s10924-019-01382-6

Majno G (1975) The healing hand: man and wound in the ancient world. Harvard University Press, Cambridge

Martins NC, Freire CS, Pinto RJ, Fernandes SC, Pascoal Neto C, Silvestre AJ et al (2012) Electrostatic assembly of Ag nanoparticles onto nanofibrillated cellulose for antibacterial paper products. Cellulose 19:1425–1436. https://doi.org/10.1007/s10570-012-9713-5

Martins NC, Freire CS, Neto CP, Silvestre AJ, Causio J, Baldi G et al (2013) Antibacterial paper based on composite coatings of nanofibrillated cellulose and ZnO. Colloids Surf A Physicochem Eng Asp 417:111–119. https://doi.org/10.1016/j.colsurfa.2012.10.042

Miles AA, Misra SS (1938) The estimation of the bactericidal power of blood. Epidemiol Infect 38(6):732–749

Montero P, Borderías J, Turnay J, Leyzarbe MA (1990) Characterization of hake (*Merluccius* merluccius L.) and trout (Salmo irideus Gibb) collagen. J Agric Food Chem 38(3):604–609. https://doi.org/10.1021/jf00093a004

Mörseburg K, Chinga-Carrasco G (2009) Assessing the combined benefits of clay and nanofibrillated cellulose in layered TMP-based sheets. Cellulose 16:795–806. https://doi.org/10.1007/s10570-009-9290-4

Mulyadi A, Zhang Z, Deng Y (2016) Fluorine-free oil absorbents made from cellulose nanofibril aerogels. ACS Appl Mater Interfaces 8(4):2732–2740. https://doi.org/10.1021/acsami.5b10985

Nechyporchuk O, Belgacem MN, Bras J (2016) Production of cellulose nanofibrils: a review of recent advances. Ind Crops Prod 93:2–25. https://doi.org/10.1016/j.indcrop.2016.02.016

Norland RR (1990) Fish gelatin. In: Voight MN, Botta JK (eds) Technomic Publishing Co., Lancaster, pp 325–333

Olsson RT, Samir M, Salazar-Alvarez G, Belova L, Strom V, Berglund LA (2010) Making flexible magnetic aerogels and stiff magnetic nanopaper using cellulose nanofibrils as templates. Nat Nanotechnol 5:584–588. https://doi.org/10.1038/nnano.2010.155

Ondaral S, Çelik E, Kurtuluş OÇ, Aşıkuzun E, Yakın İ (2018) Chitosan adsorption on nanofibrillated cellulose with different aldehyde content and interaction with phosphate buffered saline. Carbohydr Polym 186:192–199. https://doi.org/10.1016/j.carbpol.2017.12.028

Ondaral S, Hocaoğlu G, Ergün ME (2015) Cationic and anionic nanofibrillated cellulose as dry strength additives for papermaking. Cell Chem Technol 49(7–8):617–623

Osong SH, Dahlström C, Forsberg S, Andres B, Engstrand P, Norgren S, Engström AC (2016) Nanofibrillated cellulose/nanographite composite films. Cellulose 23:2487–2500. https://doi.org/10.1007/s10570-016-0990-2

Palan Abdullah MS, Noordin MI, Ismail SIM, Mustapha NM, Jasamai M, Danik MF, Ismail WAW, Shamsuddin AF (2018) Recent advances in the use of animal-sourced gelatine as natural polymers for food. Cosmet Pharm Appl Sains Malays 47(2):323–336

Pei Y, Ye D, Zhao Q, Wang X, Zhang C, Huang W, Zhang N, Liu S, Zhang L (2015) Effectively promoting wound healing with cellulose/gelatin sponges constructed directly from a cellulose solution. J Phys Chem 38:7518–7528. https://doi.org/10.1039/C5TB00477B

Powell LC, Khan S, Carrasco GC, Wright CJ, Hill KE, Thomas DW (2016) An Investigation of pseudomonas aeruginosa biofilm growth on novel nanocellulose fibre dressing. Carbohydr Polym 137:191–197. https://doi.org/10.1016/j.carbpol.2015.10.024

Qin H, Zhang Y, Jiang J, Wang L, Song M, Bi R, Zhu P, Jiang F (2021) Multifunctional superelastic cellulose nanofibrils aerogel by dual ice-templating assembly. Adv Funct Mater 31(46):2106269. https://doi.org/10.1002/adfm.202106269

Rees A, Powell LC, Carrasco GC, Gethin DT, Syverud K, Hill KE, Thomas DW (2015) 3D bioprinting of carboxymethylated-periodate oxidized nanocellulose constructs for wound dressing applications. Biomed Res Int. https://doi.org/10.1155/2015/925757

Rehm BHA, Moradali MF (2018) Alginates and their biomedical applications. Springer Nature Singapore Pte Ltd., Singapore

Rizal S, Yahya EB, Abdul Khalil EPS, Abdullah CK, Marwan M, Ikramullah I, Muksin U (2021) Preparation and characterization of nanocellulose/chitosan aerogel scaffolds using chemical-free approach. Gels 7(4):246. https://doi.org/10.3390/gels7040246

Saberi Riseh R, Gholizadeh Vazvani M, Ebrahimi-Zarandi M, Skorik YA (2022) Alginate-induced disease resistance in plants. Polymers 14(4):661. https://doi.org/10.3390/polym14040661

Saito T, Nishiyama Y, Putaux JL, Vignon M, Isogai A (2006) Homogeneous suspensions of individualized microfibrils from TEMPO-catalyzed oxidation of native cellulose. Biomacromol 7(6):1687–1691. https://doi.org/10.1021/bm060154s

Schrieber R, Gareis H (2007) Gelatine handbook-theory and industrial practice. WILEY-VCH Verlag GmbH & Co, Berlin

Sehaqui H, Mushi NE, Morimune S, Salajkova M, Nishino T, Berglund LA (2012) Cellulose nanofiber orientation in nanopaper and nanocomposites by cold drawing. ACS Appl Mater Interfaces 4(2):1043–1049. https://doi.org/10.1021/am2016766

Shieh JJ, Huang RYM (1998) Chitosan/N-methylol nylon 6 blend membranes for the pervaporation separation of ethanol–water mixtures. J Memb Sci 148(2):243–255. https://doi.org/10.1016/S0376-7388(98)00165-3

Stergar J, Maver U (2016) Review of aerogel-based materials in biomedical applications. J Solgel Sci Technol 77:738–752. https://doi.org/10.1007/s10971-016-3968-5

Straccia M, D'Ayala G, R I, Oliva A, Laurienzo P (2015) Alginate hydrogels coated with chitosan for wound dressing. Mar Drugs 13(5):2890–2908. https://doi.org/10.3390/md13052890

Struszczyk MH (2002) Chitin and Chitosan, Part II. Application of Chitosan. Polimery 47(6):396–403

Sun X, Yang Y, Yu J, Wei Q, Ren X (2024) Chitosan-based supramolecular aerogel with "skeletal structure" constructed in natural deep eutectic solvents for medical dressings. Int J Biol Macromol 254:127720. https://doi.org/10.1016/j.ijbiomac.2023.127720

Tan Y, Zi Y, Pen J, Shi C, Zheng Y, Zhong J (2023) Gelatin as a bioactive nanodelivery system for functional food applications. Food Chem. https://doi.org/10.1016/j.foodchem.2023.136265

Taokaew S, Seetabhawang S, Siripong P, Phisalaphong M (2013) Biosynthesis and characterization of nanocellulose-gelatin films. Materials 6(3):782–794. https://doi.org/10.3390/ma6030782

Vaziri AS, Alizadeh M, Vasheghani-Farahani E, Karakaya E, Detsch R, Boccaccini AR (2024) Polyethylenimine inclusion to develop aqueous alginate-based core-shell capsules for biomedical applications. ACS Appl Mater Interfaces 16(20):25652–25664. https://doi.org/10.1021/acsami.4c01186

Wang H, Gong Y, Wang Y (2014) Cellulose-based hydrophobic carbon aerogels as versatile and superior adsorbents for sewage treatment. RSC Adv 4(86):45753–45759. https://doi.org/10.1039/C4RA08446B

Wang Y, Uetani K, Liu S, Zhang X, Wang Y, Lu P, Wei T, Fan Z, Shen J, Yu H, Li S, Zhang Q, Li Q, Fan J, Yang N, Wang Q, Liu Y, Cao J, Li J, Chen W (2017) Multifunctional bionanocomposite foams with a chitosan matrix reinforced by nanofibrillated cellulose. ChemNanoMat 3(2):98–108. https://doi.org/10.1002/cnma.201600266

Wang T, Yi W, Zhang Y, Wu H, Fan H, Zhao J, Wang S (2023) Sodium alginate hydrogel containing platelet-rich plasma for wound healing. Colloids Surf B Biointerfaces 222:113096. https://doi.org/10.1016/j.colsurfb.2022.113096

Wang Y, Guo Y, Liu Y, Zhao X, Huang Y, Zhang X et al (2024) Platelet vesicles synergetic with biosynthetic cellulose aerogels for ultra-fast hemostasis and wound healing. Adv Healthc Mater. https://doi.org/10.1002/adhm.202304523

Winter GD (1962) Formation of the scab and the rate of epithelization of superficial wounds in the skin of the young domestic pig. Nature 193:293–294

Wong JC, Kaymak H, Tingaut P, Brunner S, Koebel MM (2015) Mechanical and thermal properties of nanofibrillated cellulose reinforced silica aerogel composites. Microporous Mesoporous Mater 217:150–158. https://doi.org/10.1016/j.micromeso.2015.06.025

Wu T, Farnood R, O'Kelly K, Chen B (2014) Mechanical behaviour of transparent nanofibrillar cellulose-chitosan nanocomposite films in dry and wet conditions. J Mech Behav Biomed Mater 32:279–286. https://doi.org/10.1016/j.jmbbm.2014.01.014

Wu Y, Luo X, Li W, Song R, Li J, Li B, Liu S (2016) Green and biodegradable composite films with novel antimicrobial performance based on cellulose. Food Chem 197:250–256. https://doi.org/10.1016/j.foodchem.2015.10.127

Xiao S, Gao R, Gao L, Li J (2016) Poly (vinyl alcohol) films reinforced with nanofibrillated cellulose (NFC) isolated from corn husk by high intensity ultrasonication. Carbohydr Polym 136:1027–1034. https://doi.org/10.1016/j.carbpol.2015.09.115

Yang H, Wang S, Bian H, Xing X, Yu J, Wu X et al (2022) Extracellular matrix-mimicking nanofibrous chitosan microspheres as cell micro-ark for tissue engineering. Carbohydr Polym 292:119693. https://doi.org/10.1016/j.carbpol.2022.119693

Yue C, Ding C, Hu M, Zhang R, Cheng B (2024) Collagen/functionalized cellulose nanofibril composite aerogels with pH-responsive characteristics for drug delivery system. Int J Biol Macromol 261:129650. https://doi.org/10.1016/j.ijbiomac.2024.129650

Zhang Q, Cheng Y, Fang C, Shi J (2022) Construction of novel regenerated cellulose based foam derived from waste cigarette filters as effective oil adsorbent. J Appl Polym Sci 139(14):51900. https://doi.org/10.1002/app.51900

Zhang Y, Yang Y, Zhao X, Gao J (2023) Investigation on ionical cross-linking of alginate by monovalent cations to fabrication alginate gel for biomedical application. React Funct Polym 183:105484. https://doi.org/10.1016/j.reactfunctpolym.2022.105484

Zhou J, Liu S, Qi J, Zhang L (2006) Structure and properties of composite films prepared from cellulose and nanocrystalline titanium dioxide particles. J Appl Polym Sci 101(6):3600–3608. https://doi.org/10.1002/app.22650